



Mechanical behaviors of bimsoils during triaxial deformation revealed using real-time ultrasonic detection and post-test CT image analysis

Y. Wang¹ · C. H. Li¹ · Z. Q. Hou¹

Received: 15 May 2018 / Accepted: 14 December 2018 / Published online: 28 December 2018
© Saudi Society for Geosciences 2018

Abstract

Real-time ultrasonic experiments were conducted to investigate the mechanical responses of block-in-matrix soil (bimsoil) samples under triaxial deformation. Although the mechanical behaviors of bimrocks and bimsoils have been widely studied, the rock-soil (block-matrix) interface cracking, rock-soil interaction, block occlusion, and interlocking effects during triaxial deformation are still incompletely understood. This paper aims to investigate the effect of confining pressure and block proportion on ultrasonic and mechanical properties of bimsoils using ultrasonic pulse velocity (UPV). Conventional compaction soil testing was adapted to produce cylindrical bimsoil samples of different rock block percentages (RBP) with various hammer counts, to ensure roughly the same compactness of soil matrix. The experimental results show that UPV reflects the complex mechanical behavior of bimsoils during deformation. UPV measurements became more variable as samples deformed at the pre-peak and post-peak stages. It is suggested that the UPV is affected not only by stress level but also the meso-structures that develop during failure in bimsoils. Observation of macroscopic fracture morphology combined with image analysis of mesoscopic computed tomography (CT) scans reveals that multiple localized tortuous bands form during deformation due to the presence of rock blocks in bimsoils. The changes of UPV are mainly attributed to the interactions of soil matrix and rock block. The post-test CT images further confirm this result.

Keywords Bimsoils · Mechanical behaviors · Ultrasonic testing · Triaxial compression · CT images

Introduction

The term bimrock (block-in-matrix rock) introduced by Medley (1994) is used to describe geological formations composed of a mixture of stiff rock blocks within a bonded matrix of finer texture. Due to the structural difference of the individual components, large elastic contrast exists among the rock blocks and weak matrix.

The rock block proportion and its size distribution, orientation, and spatial distributions affect the geomechanical behaviors of the mixtures at all scales of engineering interest. If the weak matrix is soil, this kind of geomaterial is often called bimsoil (block-in-matrix soil) (Medley 1994; Kalender et al. 2014; Wang et al. 2017a,b). The bimsoils are characterized by heterogeneity, environmental sensitivity, and poor block-matrix cementation. Typical bimsoils include opencast dumps, cemented waste backfills, weathered rocks, colluvium, and glacial tills, etc. These geomaterials are distributed all over the world, and often represent a challenge to engineering practitioners (Medley and Zekkos 2011). The ever-increasing importance of bimsoil in the geotechnical engineering construction has drawn more and more attention of many engineers in recent years. Given the great spatial, physical, and geomechanical variability of those stiff block and weak soil matrix mixtures, the contributions of the rock blocks on the overall strength of bimsoils are often neglected by geotechnical engineers, who may instead

✉ Y. Wang
wyzhou@ustb.edu.cn

C. H. Li
lch_ustb@126.com

Z. Q. Hou
houzq_ustb@126.com

¹ Beijing Key Laboratory of Urban Underground Space Engineering, Department of Civil Engineering, School of Civil & Resource Engineering, University of Science and Technology Beijing, Beijing 100083, China

perform designs using the mechanical properties of just the weak soil matrix. However, as indicated by many cases in the literature, series geotechnical problems can occur (Kim et al. 2004; Button et al. 2004; Tsiambaos 2010; Medley and Zekkos 2011; Tsesarsky et al. 2016). Napoli et al. (2018) used a stochastic approach to consider the content, dimensional variability, and spatial positions of rock blocks in slope stability models, their studies showed that potential inaccuracies may appear if neglecting the influence of blocks at the design stage; therefore, the bimsoil should be considered as a kind of heterogeneous material. Nowadays, the ever-increasing importance of rock block on the geomechanical behaviors of bimsoils has drawn the attention of many engineers in recent years.

The effects of rock blocks on the mechanical and physical behaviors of bimrocks or bimsoil have been widely studied by laboratory testing (Lindquist 1994; Lindquist and Goodman 1994; Akram 2010; Afifipour and Moarefvand 2014; Wang and Li 2015; Wang et al. 2015, 2016; Priyadarshie et al. 2018), large-scale in situ testing (Coli et al. 2011; Zhang et al. 2016) and numerical simulation (Zhang et al. 2015; Yongbo et al. 2015; Cen et al. 2017) on artificial and natural samples. The previous investigations have pointed out that the damage and cracking of bimsoils include behaviors such as soil-rock interface slipping, rock block movement and rotation, soil matrix cracking, and crack propagation/coalescence. However, monitoring these complicated interactions of soil matrix and rock blocks during the whole deformation process is very difficult.

Significant recent attempts have been done to monitor and map the in situ physical characteristics during sample deformation, such as the acoustic emission monitoring by Slatalla et al. (2010), who obtained the failure characteristics of bimsoil with high block proportion by investigating the initiation, propagation, and coalescence of cracks, Yamamoto and Springman (2017) conducted three and four bending test using acoustic emission monitoring, studying the ductile fracture response of frozen bimsoil, the in situ X-ray computed tomography (CT) technique to visualize the meso-structural changes at different loading stages in the stress strain curves (Wang et al., 2014, 2018), and three-dimensional laser scanning of the fracture surfaces after sample failure (Wang et al. 2016). Another effective and widely used technique is ultrasonic inspection. This technique is non-destructive and feasible to apply both to laboratory and field conditions and is commonly used to study the relationships between the strength and ultrasonic pulse velocity for rock and concrete materials (Hartmut 2001; Akkaya et al. 2003; Yasar and Erdogan 2004; Bayram et al. 2014). In addition, there are different empirical relationships for uniaxial

compressive strength (UCS) and P-wave or S-wave velocities have also been established for rock and concrete (Kahraman 2002; Su et al. 2012). From the changes of velocity, the stability of bimsoil structures can be monitored to examine the reinforcement effect and provide some significant theoretical basis for the geophysical exploration of bimsoils and bimrocks (Du et al. 2018).

Application of the ultrasonic technique to bimsoils is not common compared to experiments compared with the soil, rock, and rock-like materials. Kahraman et al. (2015) studied the volumetric block proportion (VBP) of Misis fault breccias in Adana, Turkey, using ultrasonic measurement and imaging techniques and the correlation of VBP and P-wave and S-wave UPV was studied. Mahdevari and Maarefvand (2017) used the ultrasonic experiments to evaluate the block content in bimsoils and developed a relationship between the volumetric block proportion and P-wave and S-wave velocities. Wang et al. (2015) performed experiments on bimsoils in which the ultrasonic and mechanical characteristics were studied: ultrasonic measurement was used for bimsoil with different block proportions and block shapes under uniaxial compression, the experimental results show that UPV decreases with increasing rock percentage for all samples; in addition, UPV has a fluctuation growth trend with increasing of axial stress. The results confirm that the ultrasonic and mechanical properties of bimsoil are closely related to rock block proportion. Moreover, the cracking damage mechanism has been proposed based on the changes of UPV with total crack widths (Wang et al. 2015), from the variation of crack width during sample deformation, the damage behaviors were divided into three stages. For the bimsoil under splitting loading, Wang et al. (2017b) developed the correlations between tensile stress and UPV that have been revealed by investigating the macro-meso failure mechanism using real-time ultrasonic measurement and 3D laser scanning.

In this study, we continue to study the mechanical behaviors of bimsoil through laboratory experimentation. Unlike in our previous studies, recent bimsoil experiments were carried out using triaxial compressive stress paths. A novel experiment system was devised which included a special custom-designed loading device combined with ultrasonic measurement techniques. Rather than focus on the macroscopic stress-strain characteristics, this paper explores the UPV characteristics and the UPV-pressure correlation during the whole deformation process. The structural change of bimsoil is investigated from the variation of UPV. After the ultrasonic testing, X-ray computed tomography (CT) scanning and image analysis were used to visualize the fracture pattern and further reveal the mesoscopic failure mechanism of the examined bimsoil.

Table 1 Soil properties in bimsoil from laboratory physical and mechanical testing

Index	Soil matrix	Rock block
Natural density (g/cm^3)	1.66	2.67
Dry density (g/cm^3)	2.03	/
Natural water content (%)	20.2–23.1	
Optimum water content (%)	9.5	/
Relative density (G_s)	2.73	/
Uniformity coefficient, C_u	4.2	/
Coefficient of curvature, C_c	1.32	/
Liquid limit (%)	64	/
Plastic limit (%)	36	/
Plasticity index, W_p	28	/
Liquidity index, W_L	0.121	/

Samples and testing procedure

Characteristics of materials used in bimsoil

(1) Aggregate

For the ultrasonic testing, bimsoil cylindrical samples were prepared with size of 50 mm diameter (Φ) and height (H) of 100 mm. Referring to a sampling standard in GB/T 50123-1999 (MWRPRC 1999), the threshold value for rock-soil phase is determined as 2 mm, and diameter of blocks should be less than 1/5 the sample diameter (i.e., 10 mm). The rock blocks were supplied from crushed marble aggregates with a diameter of 4–8 mm. The uniaxial compressive strength (UCS) and elastic modulus (E) of the rock block were determined by conducting laboratory uniaxial compression test. The UCS of the rock block is 94.5 MPa, and elastic modulus was 23 GPa. The P wave ultrasonic pulse velocity was about 5200 m/s.

(2) Soil matrix

The weak soil matrix was taken from a reservoir foundation pit at a depth of 15 m. Based on the results of laboratory sieving test, the soil matrix was characterized as high-plasticity clay. The basic physical parameters are listed in Table 1. For the soil matrix, a method of X-ray power diffraction (XRD) was used to further reveal the mineral composition and content. The XRD tests further revealed three kinds of clay minerals, such as illite, montmorillonite, and kaolinite, in the proportions of 8.01%, 55.78%, and 36.21%, respectively.

Sample preparation

For the present investigation, the soil compaction technique was used to prepare remolded samples (Donaghe and Torrey 1994; Wang et al. 2016). From relations between the sample density and the compaction test hammer counts, the optimal hammer count for the sample preparation was determined accordingly. During bimsoil sample preparation, the rock block percentage (RBP) values were designed to be 20%, 30%, 40%, and 50% (mass ratio), respectively. By compaction testing, the optimum moisture content was determined as 9.5%. In order to keep the same density of the soil matrix for samples with different block proportions, different hammer counts were applied to the mixtures according to the relations of soil density against hammer count, as shown in Fig. 1a. The optimal hammer counts for the sample with RBP of 20%, 30%, 40%, and 50% are 8, 18, 24, and 32 times, respectively, as shown in Fig. 1b.

The required soil matrix and blocks for each bimsoil sample were blended mix for a few minutes. The mixture was then poured into a cylindrical shaped cast iron mold with an inside size of Φ 50 mm \times H 100 mm (the same as the bimsoil required sample). The sample was prepared using the

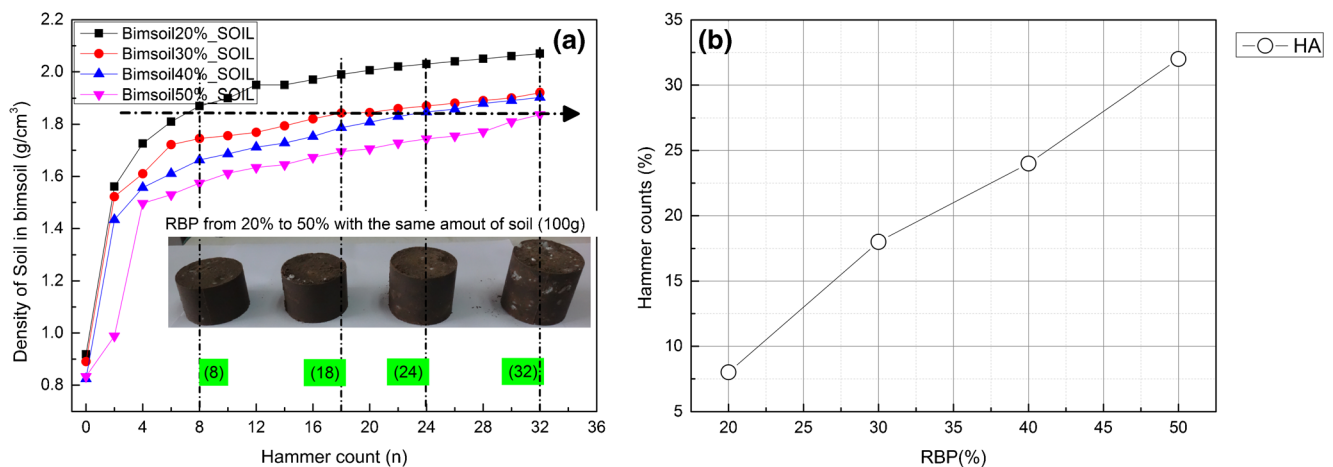


Fig. 1 Determination of hammer count for bimsoil sample with different RBPs. **a** Plot of the density of soil matrix against hammer counts. **b** Plot of the hammer count and RBP for bimsoil sample

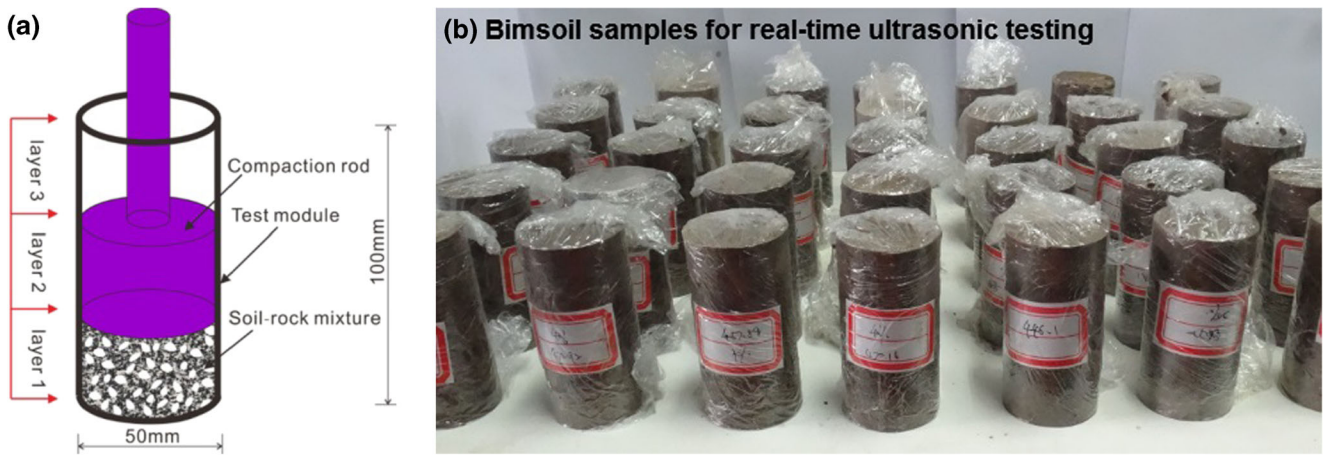


Fig. 2 Preparation of bimsoil samples for variable-angle shear test. **a** Schematic of compaction test procedure used to produce samples. **b** Air-dry bimsoil samples for the test wrapped in kitchen wrap to preserve moisture

compaction method with three layers, as shown in Fig. 2a. Before placing mixture into the next layer, the surface of the compacted layer was disturbed to a depth of about 5 mm to ensure a good connection between layers. Then, the bimsoil samples were placed in the shade to air dry.

Testing system

The testing system for the real-time ultrasonic experiment included a loading device, a pair of ultrasonic transducers,

an ultrasonoscope, and triaxial Hoek Cell to apply confining pressure, as shown in Fig. 3. The loading device is mainly composed of a rigid column, guide bar, load controller, force sensor, hydraulic jack, and micrometer gauge, etc. The axial stress and axial deformation can be read from the load controller and micrometer gauge, the precision being 0.01 kN and 0.001 mm, respectively. The ultrasonic transducer is the key component of the testing system: it includes a transmitter and a receiver. The frequency of the transducers was selected as 300 kHz, and they are specially designed to have

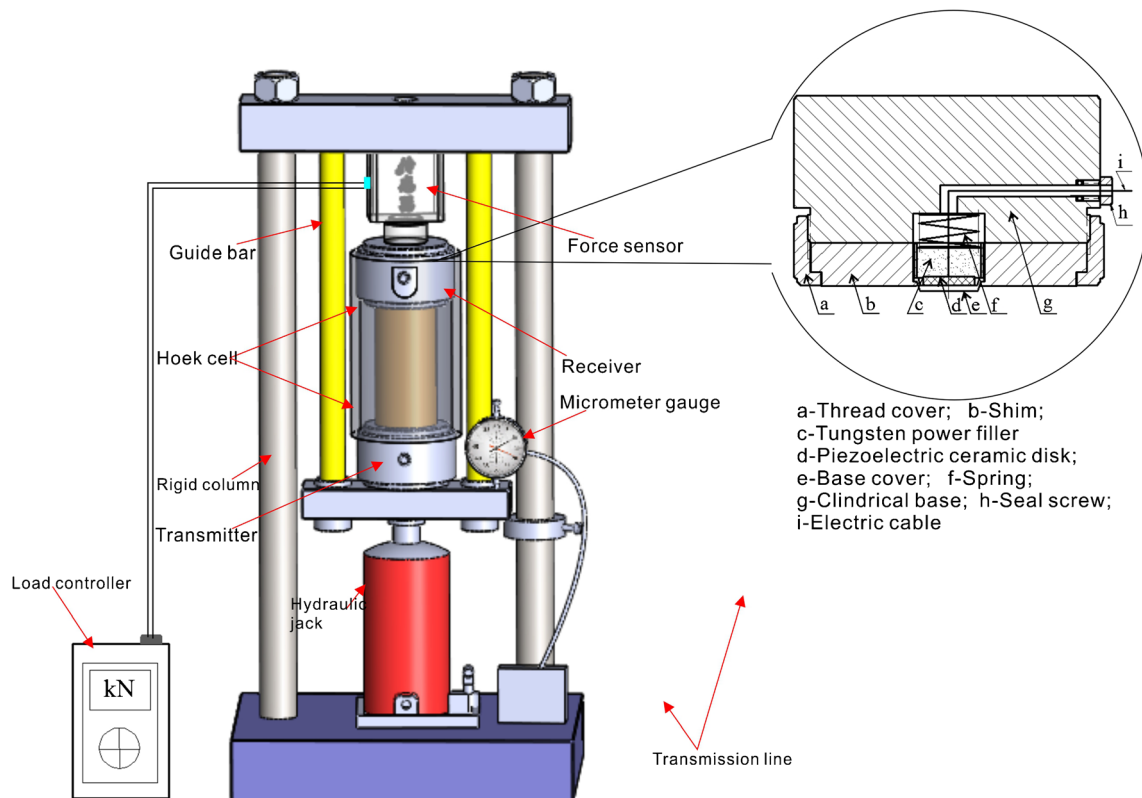
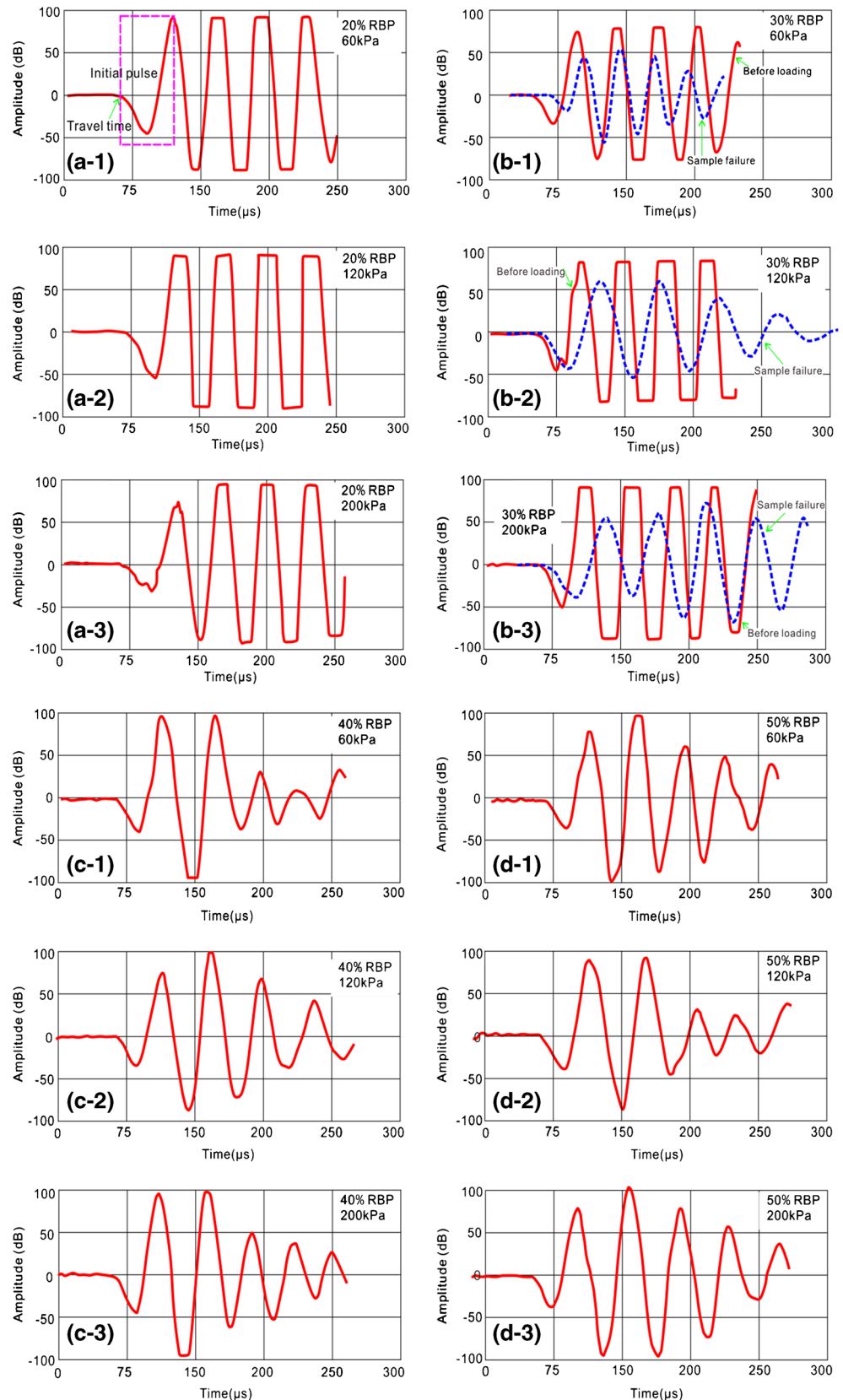


Fig. 3 The real-time ultrasonic testing system for the bimsoil sample under triaxial deformation

a flexible contact pressure head, in order to keep in close contact with the bimsoil sample. The components of the

ultrasonic transducer included thread cover, shim, tungsten power filler, piezoelectric ceramic disk, base cover, spring,

Fig. 4 The ultrasonic wave for bimsoil sample under different confining pressure. **a~d** The designed RBP is 20%, 30%, 40%, and 50%, respectively. The label “1, 2, 3” indicates the confining pressure of 60 kPa, 120 kPa, and 200 kPa



and cylindrical base, etc. The role of the ultrasonoscope was to record the ultrasonic wave; the travel time and wave amplitude can be read from the P-wave: the reading accuracy of ultrasonic wave is 0.05 μ s, the basic frequency is 20 MHz, the sampling interval ranges from 0.05 to 4000 μ s. During the test, the contact surface between the transducers and the bimsoil sample was coated with a thin film of coupling agent, to ensure full contact and removal of any voids.

Confining pressure (CP) was applied to the bimsoil sample by using a specially designed Hoek Cell with a gasbag in it. The CP value can be read from the gas-pressure gauge: the measuring range is 600 kPa, and the accuracy is 0.5 kPa. The tested bimsoils contained a larger number of random block-matrix contacts with geomechanical interfaces because of the elastic contrasts between soil matrix and rock blocks. In the process of sample deformation, the stress distribution inside the bimsoil was considered extremely uneven, the stresses were unequal on the surface of the sample. Therefore, the gasbag confining pressure system which can apply flexible boundary stress on the bimsoil sample was used to ensure a uniform stress loading condition.

Testing procedure

During the test, the sample was installed into the Hoek Cell first; the top and bottom end of the sample was connected with the ultrasonic transducers. The through-transmission (T-T) mode was used to ultrasonically inspect the sample. Then, the Hoek Cell was placed on the loading device; an axial loading rate of 0.01 kN/s was applied to the sample. In the meantime, the axial displacement, ultrasonic travel time, amplitude, and wave were recorded simultaneously. The UPV was calculated as the ratio of sample length (L) to travel time (t), as $V_P(L,t) = L/t$.

It is known that the first periodic wave is stable and reproducible under the same ultrasonic sensor and contact condition. The initial pulse was easily identified from the waves arriving later when propagating through the samples and the later waves cannot cause contamination of the first periodic wave. For this reason, the first periodic wave was usually chosen as the initial wave to obtain the travel time and amplitude. As shown in Fig. 4a~d, it plots the receiving waveform for bimsoil samples before loading, with different block proportion, and under confining pressure of 60 kPa, 120 kPa, and 200 kPa, respectively.

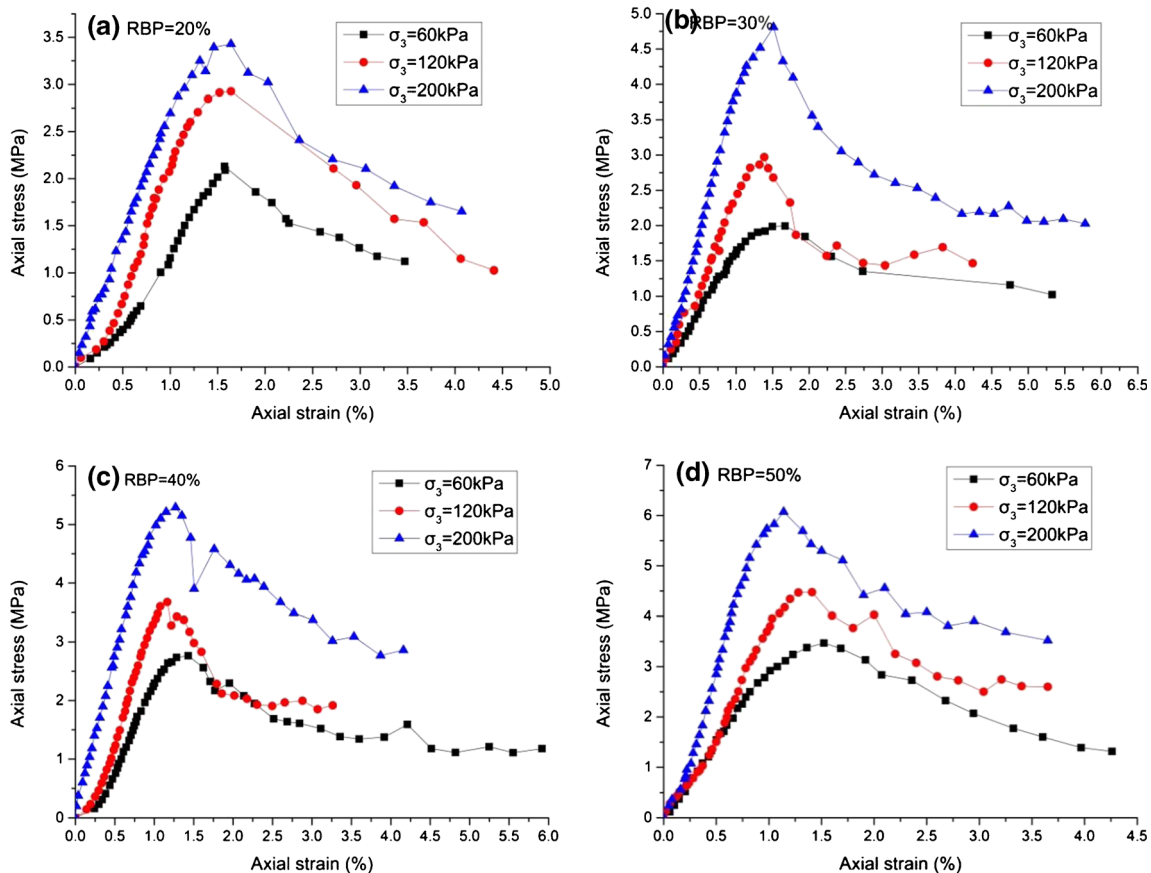


Fig. 5 The triaxial stress strain responses for bimsoil samples with different rock block proportions. **a~d** The RBP is 20%, 30%, 40%, and 50%, respectively

The repeated display of the waveform indicates repeatedly triggered in the expected interval and shows a consistent reading. The travel time and amplitude can be obtained from the initial pulse.

Results and discussions

Triaxial stress strain curves

Figure 5 depicts the typical triaxial stress strain responses for the tested bimsoil samples. The curves present strain-softening characteristics. For a sample with a certain rock proportion, the peak stress increases with the increase of confining pressure. The peak stress is the maximum for the sample with a RBP of 50% (approximately 6 MPa), and it is the minimum for the sample with a RBP of 20% (approximately 3.5 MPa). From the stress strain curves, it can be also seen that peak stress for all bimsoils tested increases with increase in confining pressure. It is interpreted that for a sample under a high confining pressure, the motion of rock blocks in bimsoil sample is limited, the skeleton formed by rock blocks plays a best role to improve the sample strength; in addition, for bimsoil samples with high rock block proportion, the interlocking among the rock blocks further enhances the

overall stiffness of bimsoil, all these effects result in the improvement of sample strength.

UPV analysis during deformation

To analyze the variation of UPV during sample deformation and facilitate the study of the changes of UPV against axial stress, the relationships between the UPV, axial stress, and axial strain are plotted in Figs. 6, 7, 8, and 9. From the experimental results, the following important findings can be obtained:

- (1). The most striking phenomenon that can be observed is that the UPV curves present variation trend with the increase of axial strain. Variation of UPV indirectly reflects the changes of density in bimsoil sample occurring during deformation. This result implies that the compactness is influenced by the interactions between the rock blocks and soil matrix. The non-linear mechanical behaviors of block movement and rotation alter the compactness of bimsoil. A series of non-linear mechanical behaviors occur during deformation, including soil consolidation, rock-soil interface cracking, block movement, crack propagation, and contact and separation repeatedly between the weak matrix and stiff blocks.

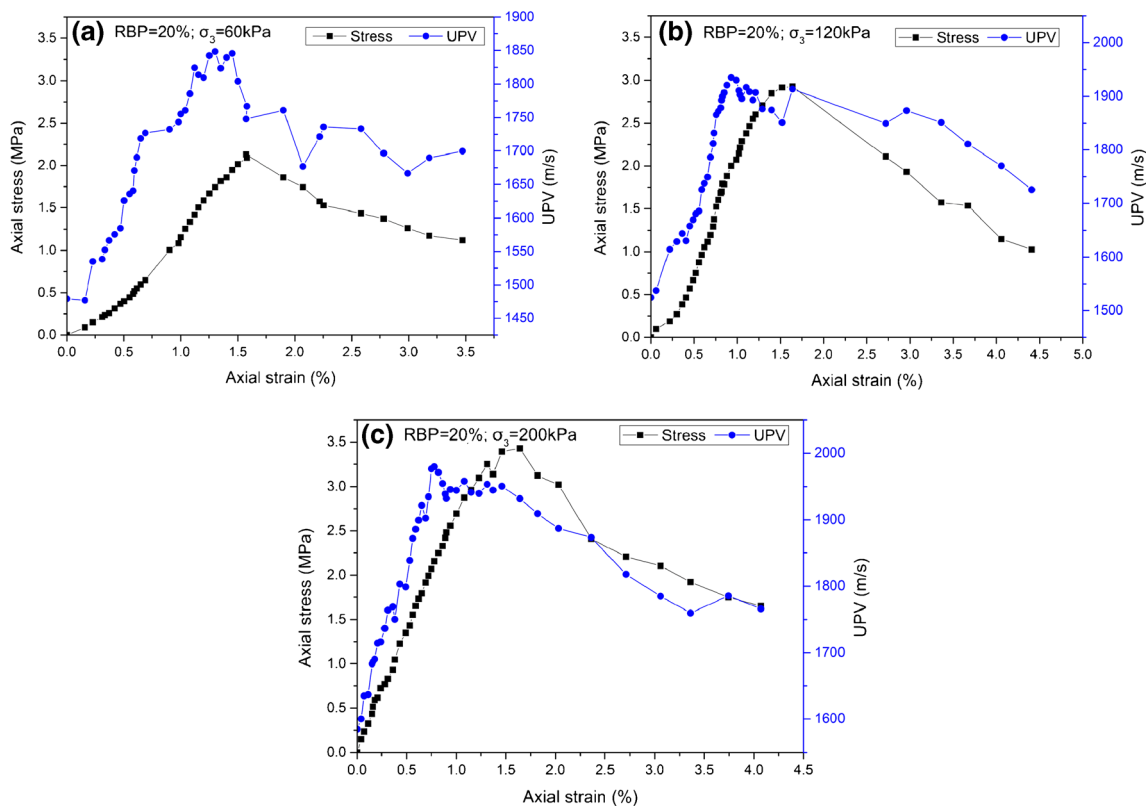


Fig. 6 Plot of the UPV and axial stress against axial strain during sample deformation for bimsoil samples with RBP of 20%. a–c The confining pressure is 60 kPa, 120 kPa, and 200 kPa, respectively

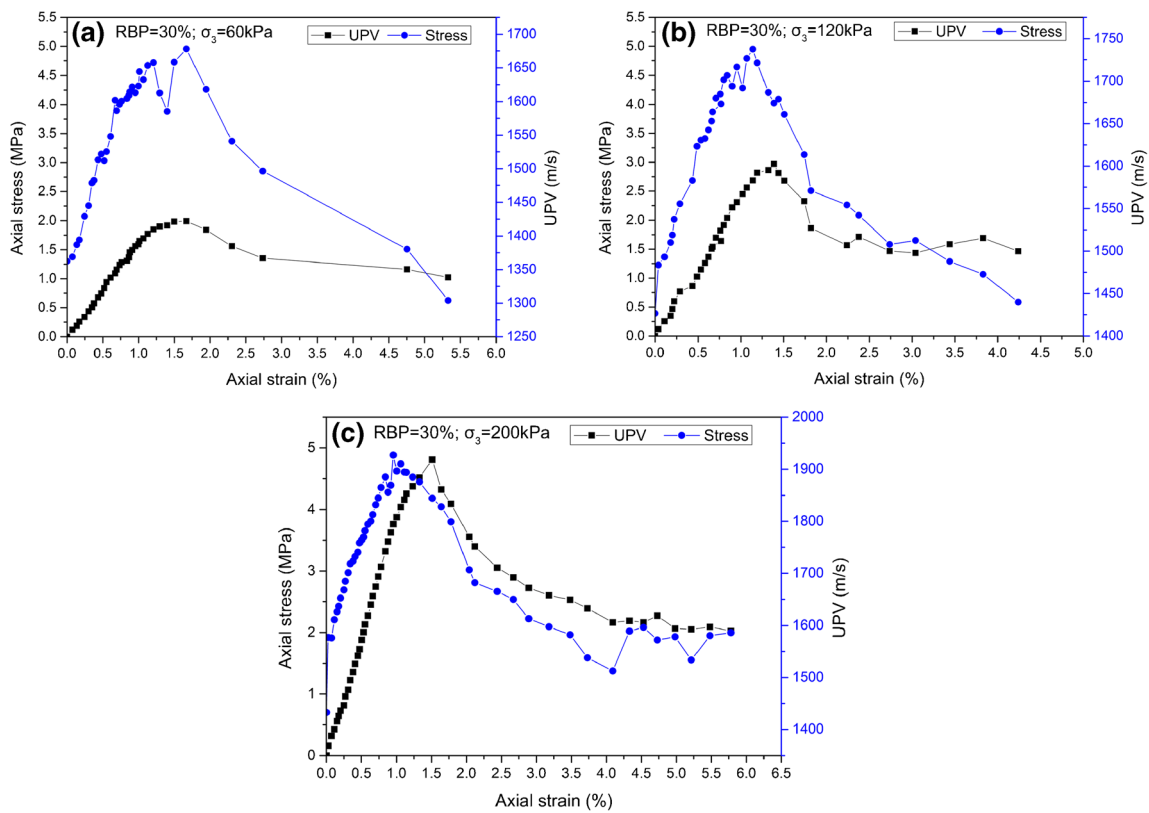


Fig. 7 Plot of the UPV and axial stress against axial strain during sample deformation for bimsoil samples with RBP of 30%. a~c The confining pressure is 60 kPa, 120 kPa, and 200 kPa, respectively

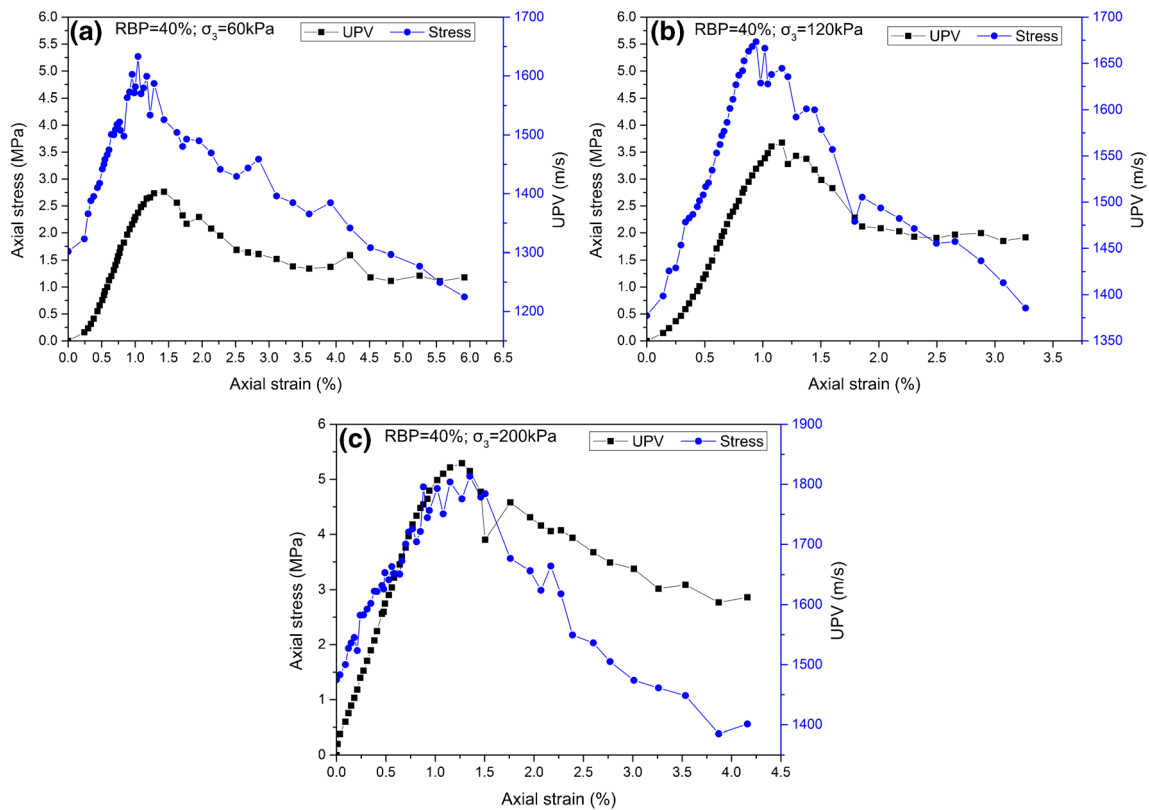


Fig. 8 Plot of the UPV and axial stress against axial strain during sample deformation for bimsoil samples with RBP of 40%. a~c The confining pressure is 60 kPa, 120 kPa, and 200 kPa, respectively)

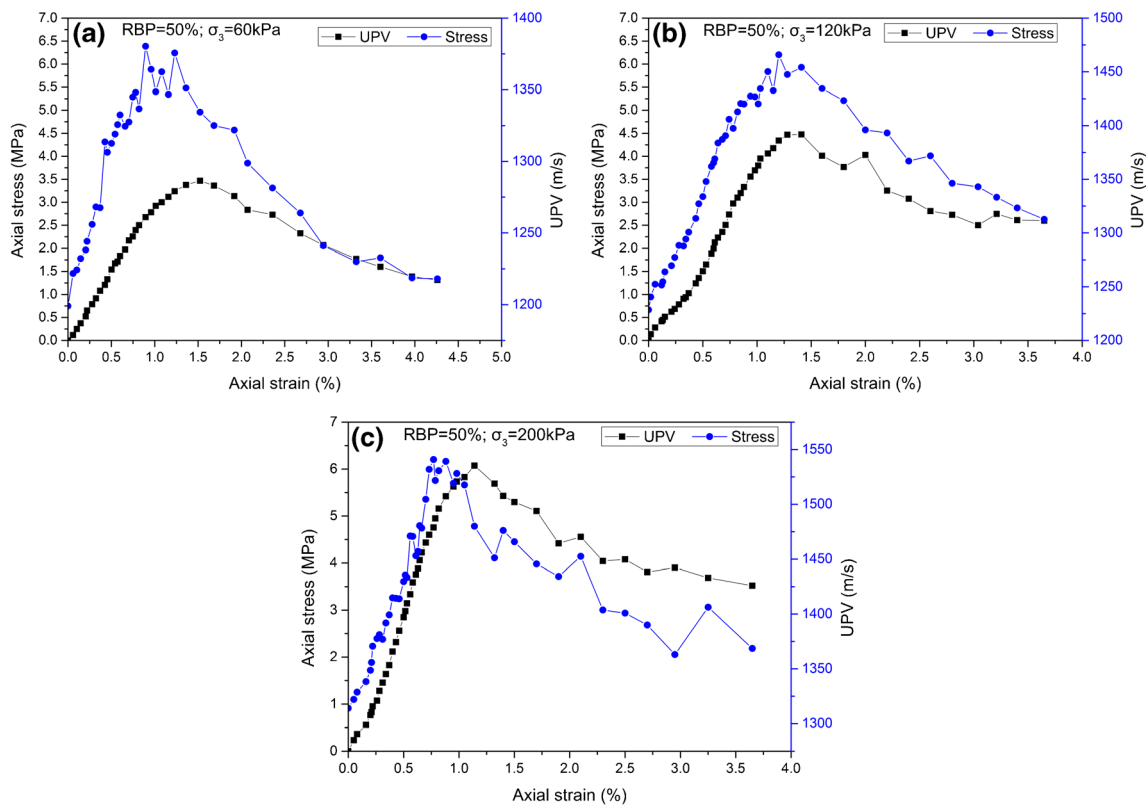


Fig. 9 Plot of the UPV and axial stress against axial strain during sample deformation for bimsoil samples with RBP of 50%. a~c The confining pressure is 60 kPa, 120 kPa, and 200 kPa, respectively)

- (2). The UPV curves indicate an increasing trend as the applied confining pressure grows. The result indicates that the degree of bounding between soil matrix and rock blocks increases at relatively high stress condition. In addition, for the samples under the same confining pressure, UPV shows a decreasing trend with the increase of block proportion. This result may be attributed to the differential acoustic impedance for the components (e.g., soil, block, pore, crack, etc.) in bimsoil sample; the diffraction and scattering effects result in the increment of travel time for the sample with high block content. Secondly, due to the existence of the complex stochastic interfaces in bimsoil, such as rock-soil interfaces, scattering attenuation is severe when ultrasonic wave goes through the sample, resulting in a great loss of ultrasonic energy. Thirdly, adding rock blocks in soil matrix, the propagation path increases with the increasing of block proportion and this causes increased travel time. Generally then: the meso-structural heterogeneity in bimsoil and the randomly distributed rock-soil interfaces results in lengthening ultrasonic propagation paths and the reduction of the transmission energy. All the above factors cause of travel time to increase when ultrasonic waves pass bimsoil.
- (3). Post-peak stress, UPV decreases but not to zero. The variation trend of UPV against axial stress is different from the experimental result of Wang et al. (2015), in their studies, the UPV of bimsoil decreased to zero under uniaxial compression. The result indicates that although the entire sample is destroyed, bonding effects between the rock block and soil matrix survive. The stress strain curve also shows a phenomenon that residual strength exists for bimsoil, the skeleton of rock blocks resists deformation, so the UPV can still be measured at this stage.
- (4). From the pre-peak curves of UPV, it is apparent that UPV of bimsoil increases with increasing normal stress, but the incremental rate decreases gradually as the normal stress increases. At low stress level, the degree of block-soil bounding is relatively weak and UPV increases quickly; however, the degree of bounding decreases at high stress level owing to the compactness of sample, and the incremental rate of UPV slows down.
- (5). The UPV curves show that the fluctuation of UPV is the most obvious near the peak stress. At this stress level, the rock block and soil matrix interaction is strong, and the movement and rotation of blocks are the most serious.

Analysis of dependency of velocity to stress

As stated above, the UPV is strongly influenced by the stress state. In spite that, at a given stress level, the internal structures of sample also affected the evolution of UPV during sample deformation. In order to obtain the UPV value at any stress level, a curve fitting method is often used (Kem and Tubia 1993; Wang et al. 2015). When the curve fitting approximations were executed to study the relationship of UPV and axial stress, we can deduce the UPV at high geostatic stress. Kem and Tubia (1993) used linear curve fitting approximation to obtain the pressure coefficient, but only can fitting the experimental data at relative high stress level where the linear relationship of UPV and axial stress is good, disregarding some experimental data when the nonlinear UPV increases due to closure of cracks. In this study, a power fitting function (not linear) fitting equation was used and shown to fit the experimental data where the UPVs present nonlinear variation trend due to the interactions between the stiff blocks and weak matrix. Figures 10 and 11 depict the curve fitting results for bimsoil samples with different RBPs at the pre-peak and post-peak axial stress stages, respectively. Tables 2 and 3 list the detailed fitting parameters for the samples. It can be seen

that UPV shows a decrement trend as RBP increases; it indicates that the ultrasonic energy decreases when the wave goes through the sample with high block proportion, which results in the increasing of travel time.

Correlation of RBP and strength parameters

Mohr’s strength parameters (c , φ) of bimsoil samples with different RBPs were obtained, as listed in Table 4. The relationship between the shear strength and RBP is shown in Fig. 12. The friction angle shows an increase with the increase of RBP and cohesion decreases with RBP. Fitting results indicate that a power function relationship and a linear relationship exist for them. The correlation coefficient is 0.913 and 0.974, which indicates high correlation of the shear strength parameter and RBP. The results imply that the shearing characteristics of bimsoil are controlled by the interactions between the soil matrix and rock blocks. The experimental results of Lindquist and Goodman (1994), Coli et al. (2011), Sonmez et al. (2004), and Sonmez et al. (2006), they also found that adding rock blocks into soil matrix leads to the increase in friction angle and decrease in cohesion. The ultrasonic velocity-axial stress analysis shows a fluctuation

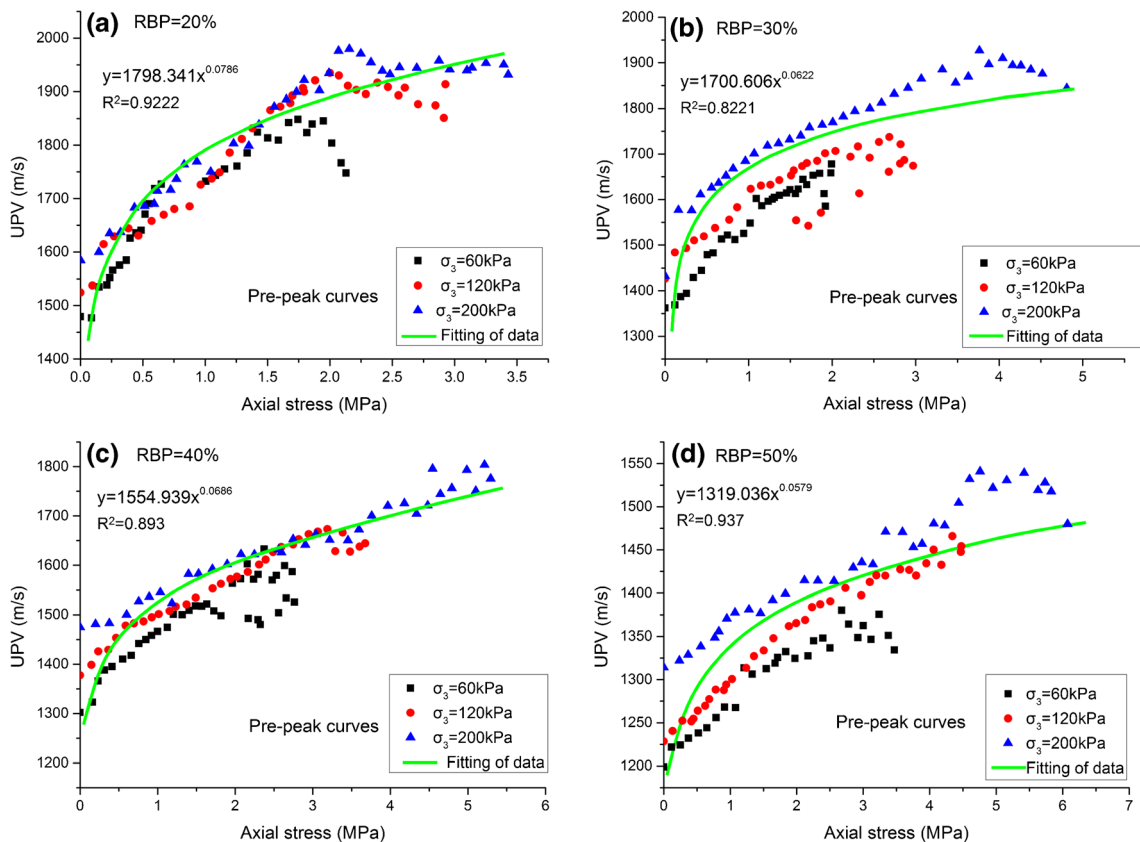


Fig. 10 The relationship between the UPV and pre-peak axial stress of the tested bimsoil samples under three confining pressures. **a–d** The RBP are 20%, 30%, 40%, and 50%, respectively

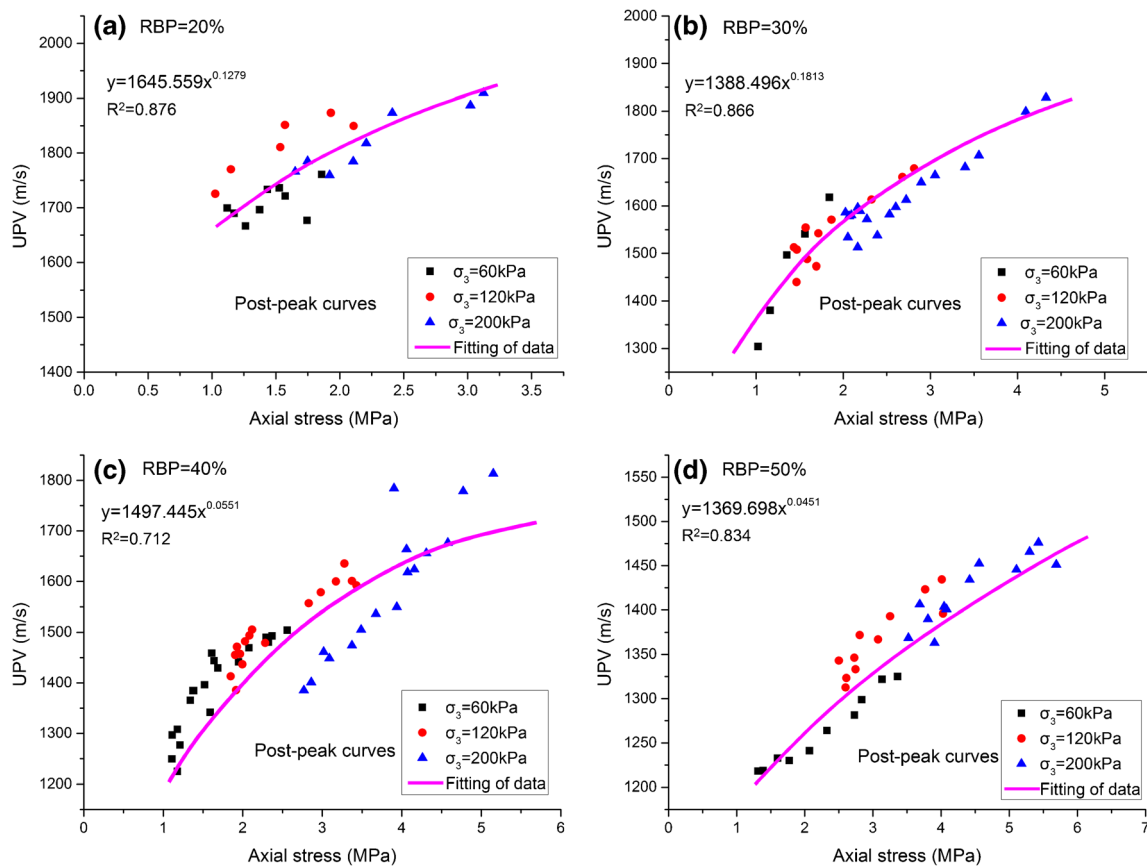


Fig. 11 The relationship between the UPV and post-peak axial stress of the tested bimsoil samples under three confining pressures. **a–d** The RBP are 20%, 30%, 40%, and 50%, respectively

increasing trend with sample deformation which reflects the complex interactions between blocks and soil matrix with the variation being more obvious near the peak stress. At the strain softening stage, for bimsoil sample with high RBP and under low confining pressure, the variability UPV becomes more apparent, which indicates stronger indicating stronger rock-soil interactions. For bimsoil sample with high rock block proportion, the interlocking and frictional effect among the blocks further result in the increment of internal friction angle. However, for the samples with low RBPs, although very little block interlocking exists, the strength increases

may be attributed to the geomechanical effects related to propagation of tortuous failure surfaces.

Analysis of failure mechanisms

The post-test failure morphology of bimsoil samples was observed visually. Figure 13 shows the samples after the test and the sketch map of cracks on sample surface. The failure morphology indicated that the failure mechanism of bimsoil was much more complicated than the pure soil and rock materials, as shown in Fig. 14. The crack patterns are complex due to the

Table 2 The fitting equations of the pre-peak axial stress and UPV, for the bimsoil samples with different RBPs

RBP (%)	Axial stress (MPa)	UPV (m/s)	$V_p = ax^b$		R^2
			a	b	
20	0~3.44 MPa	1479~1980	1798.341	0.0786	0.922
30	0~4.83 MPa	1362~1910	1700.606	0.0622	0.822
40	0~5.32 MPa	1302~1820	1554.939	0.0686	0.893
50	0~6.08 MPa	1200~1540	1319.036	0.0579	0.937

Table 3 The fitting equations of post-peak axial stress and UPV, for the bimsoil samples with different RBPs

RBP (%)	Axial stress (MPa)	UPV (m/s)	$V_p = ax^b$		R^2
			a	b	
20	1.11~3.12 MPa	1666~1910	1645.559	0.1279	0.876
30	1.02~4.33 MPa	1304~1830	1388.496	0.1813	0.866
40	1.17~5.15 MPa	1224~1814	1497.445	0.0551	0.712
50	1.31~5.69 MPa	1218~1478	1369.698	0.0451	0.834

Table 4 Strength parameters calculated for the bimsoil samples with different RBPs

RBP (%)	Internal friction angle (°)	Cohesion force (MPa)
20	54.53	0.256
30	63.85	0.181
40	65.07	0.072
50	70.45	0.021

existence of rock blocks: tensile cracks and shear crack co-exist, indicating that the fracture mechanism of bimsoil sample is due to mixed shear and tensile modes. The shape of cracks is not straight and shows multiple tortuous propagation paths. It can be referred that the failure surfaces exhibit curved shapes and negotiate rock blocks. With increases of block proportion in bimsoil sample, the number and scale of cracks increase accordingly.

In order to further reveal the fracture mechanisms, the X-ray CT tomography (CT) method was used to visualize the

crack pattern inside the bimsoil samples. Taking for example the sample with a RBP of 30% and a confining pressure of 120 kPa, Fig. 15 shows the 2D reconstructed CT images. The scanning positions were located at 20 mm (from the sample bottom) to 80 mm (20 mm below sample top). The scanning interval was set to 10 mm, and a total of seven images were obtained for each sample. Image analysis of the CT scans was performed. During extraction of the cracks and rock block features from the images, an algorithm named “median filter” was used first, in order to discriminate object boundary. Median filtering is particularly useful for reducing speckle noise, salt, and pepper noise. The edge-preserve nature of this algorithm makes it effective in detecting obscure edges, such as the irregular cracks in bimsoil. The filtering algorithm analyzed the value of each output pixel as the value of the neighborhood of the corresponding input pixel. As an example, the extracted rock blocks and cracks for the RBP = 20%/CP = 120 kPa sample are shown in Fig. 15. The CT images reveal that the crack patterns are influenced by positions of rock blocks—most of the cracks propagate around rock blocks.

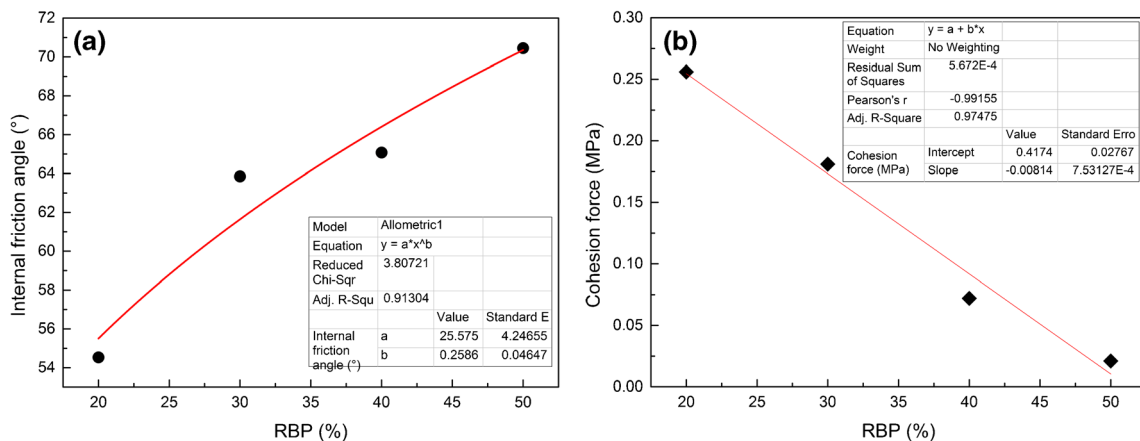


Fig. 12 Correlation between the internal friction angle (a), cohesion force (b), and rock block percentage (RBP)

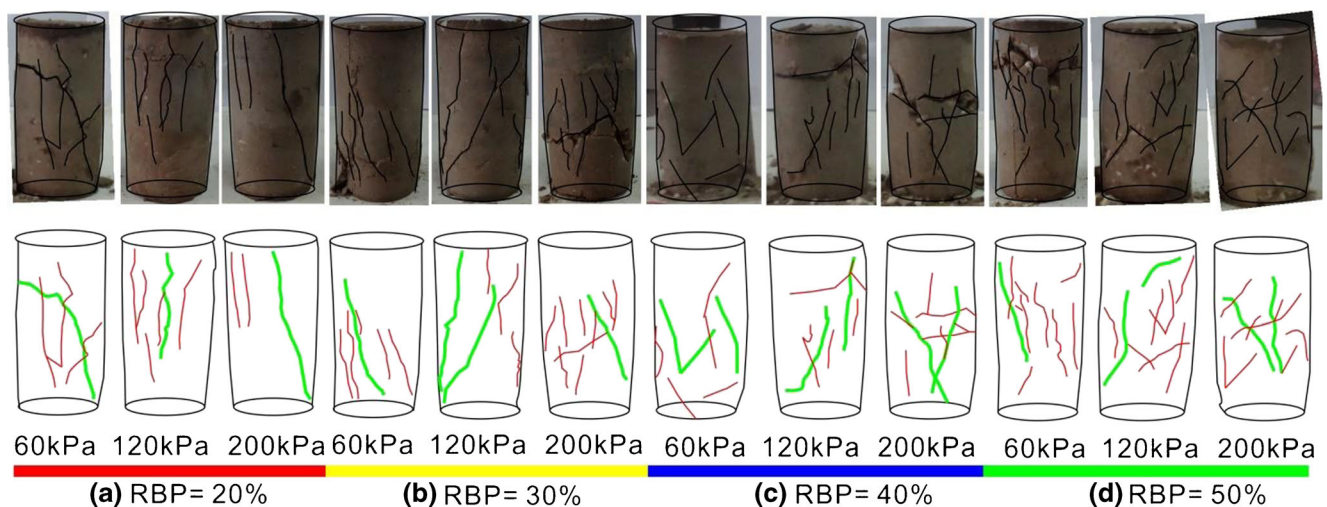


Fig. 13 The failure morphology of bimsoil samples post the real-time ultrasonic test

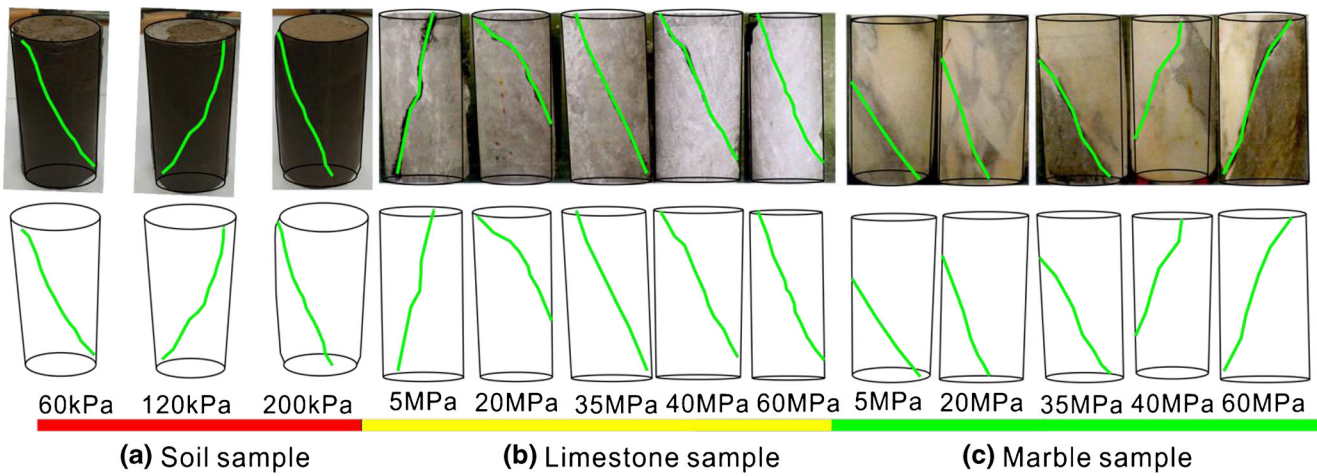


Fig. 14 Typical failure morphology of soil sample and rock sample under triaxial compression. The soil triaxial compression testing was done by the author, the rock triaxial compression testing was cited from Zhang (2016)

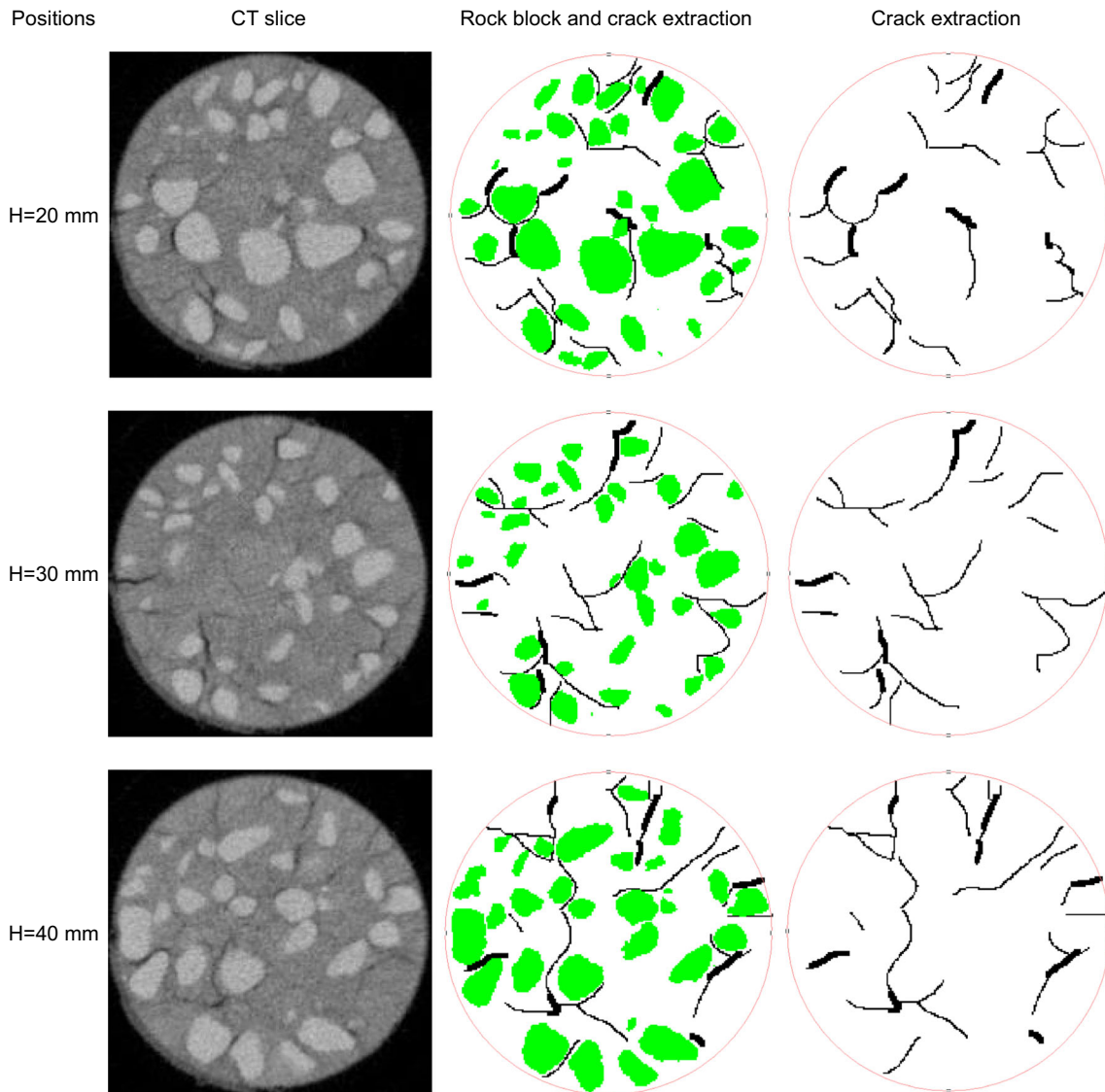


Fig. 15 The reconstructed CT images for a bimsoil sample after ultrasonic testing, the rock block and crack are extracted

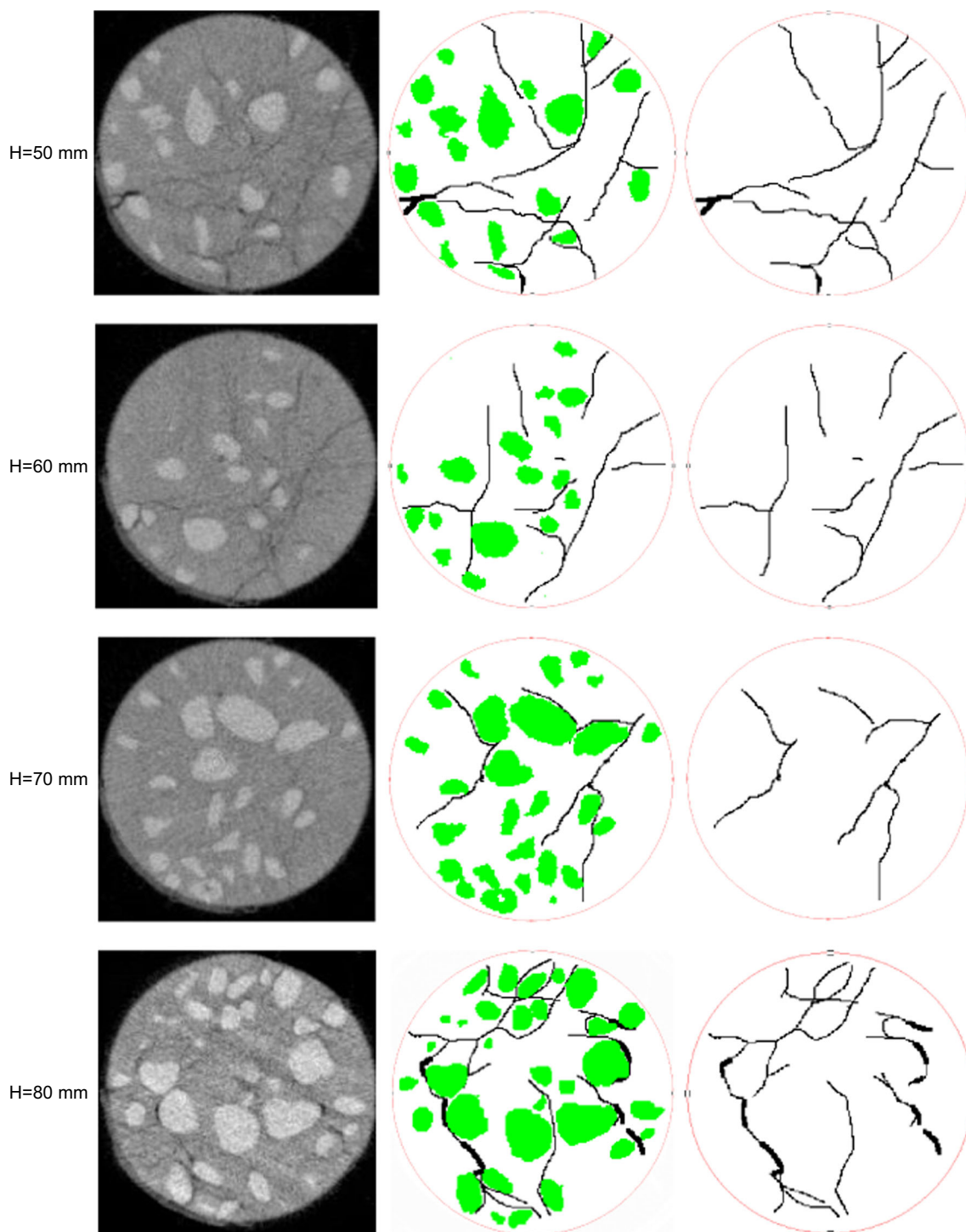


Fig. 15 continued.

Also, cracking initiates from rock-soil interface owing to the high stiff contrasts between the rock blocks and soil matrix. The nonuniform distribution of cracks indicates the characteristics of strain localizations in bimsoil samples. Localized bands may form in multiple tortuous planes, the shapes being related to the block distribution, block shapes, block sizes, and block orientations. From the CT image, the failure mechanism

of bimsoil may be apparently different from the behaviors for pure soil and rock material, indicating that the role of rock blocks control the failure pattern. Two kinds of cracks can be seen from the images, they are the main crack (green color in Fig. 13) which bypasses rock blocks and propagates into soil matrix, and the secondary crack which initiates and propagates around the blocks (red lines in Fig. 13).

Discussions

Bimsoil as heterogeneous geomaterial is mainly composed of mixtures of stiff rock blocks and relatively weak soil matrix. Many laboratory testing and numerical simulations have shown that stress distributions, strain localizations, and failure patterns of bimsoil are different from the general geomaterials of rock and soil. In this study, real-time ultrasonic measurements were obtained to investigate the mechanical behaviors of bimsoils under triaxial deformation. The non-linear mechanical response during deformation can be attributed to the interactions between soil matrix and rock blocks, which are also reflected in the variations of UPV during failure. A series of non-linear mechanical responses, such as soil compaction, rock-soil interface cracking, rock block movement, etc., change the transmission responses of ultrasonic waves, resulting in changes in travel time and the associated UPVs. Interestingly, UPV values fluctuated considerably during the whole deformation process, both at the pre-peak and post-peak stages of triaxial failures, as indicated by the corresponding stress strain curves. The degree of coupling of soil matrix and rock blocks is related to the mechanical state of the bimsoil sample during deformation. Our experiment results further indicated that the ultrasonic characteristics of bimsoil are not only affected by the stress level but also by internal structural factors. The failure morphology of samples was studied using both visual observation of the surface of failed specimens, as well as X-ray CT images. Multiple localized shear bands were visualized which apparently were affected by the rock blocks. Because of the stiffness contrast between the matrix and block, cracking always occurs at the relatively weak soil-rock interfaces, and then cracks negotiated the rock blocks in a tortuous fashion to propagate into the soil matrix. The distribution, orientation, and shape of rock blocks affect the propagation path of cracks apart from the stress state, which can be seen from the CT images.

The analysis of stress-UPV dependency is significant to the estimation of slope stability evaluation of reinforcement effect of blocks in soil masses, and the possible future geophysical exploration of in situ bimsoils. Our experimental results show that ultrasonic technique is an effective tool to understand the mechanical state and behaviors of bimsoils at the laboratory scale. In the future study, more ultrasonic parameters (e.g., attenuation coefficient, quality factor, dominant frequency, etc.) should be used to explore the mechanical behaviors of bimsoil.

Conclusions

A specially designed and fabricated testing system was used to perform real-time ultrasonic testing for bimsoil samples under triaxial deformation. Remolded bimsoil samples with various

proportions of rock blocks were prepared to roughly ensure the same soil compactness in the experiment. The variations of UPV during the whole process were obtained as well as CT scanning and image analysis. The main conclusions are summarized as below:

- (1). As a reliable, sample, and practical nondestructive technology, experimental results indicate that the real-time UPV testing can be used in the laboratory to study the mechanical responses of bimsoil during deformation. The mechanical and ultrasonic characteristics of bimsoil are closely related to the meso-structures and stress state.
- (2). Complicated mechanical behaviors of bimsoils during deformation can be indirectly reflected by the variations of UPV. The internal meso-structures of bimsoil sample, along with the stress levels, affect the transmission properties of ultrasonic waves. The increasing trend of sometimes greatly fluctuating UPV measurements in the pre-peak stage reflects the mechanical interaction between soil and rock block.
- (3). Macroscopic fracture morphology description and mesoscopic CT image analysis revealed the failure mechanism of bimsoil. Localized deformation is controlled by the rock blocks and multiple tortuous failure surfaces may form due to the influence of the rock blocks. The CT images supported the mechanical response analysis inferred by the ultrasonic testing.

Acknowledgements The authors would like to thank the editors and the anonymous reviewers for their helpful and constructive comments.

Funding information This work was supported by the National key technologies Research & Development program (2017YFC0804103, 2018YFC0808402, 2018YFC0604601), the Fundamental Research Funds for the Central Universities (2302017FRF-TP-17-027A1), the National Natural Science Foundation of China (Grants Nos. 41502294), and the State Key Laboratory for GeoMechanics and Deep Underground Engineering, China University of Mining & Technology (SKLGDUEK1824),

Compliance with ethical standards

Conflict of interest The authors declare that they have no conflict of interest.

References

- Afifipour M, Moarefvand P (2014) Failure patterns of geomaterials with block-in-matrix texture: experimental and numerical evaluation. *Arab J Geosci* 7:2781–2792
- Akkaya Y, Voigt T, Subramaniam KV (2003) Nondestructive measurement of concrete strength gain by an ultrasonic wave reflection method. *Mater Struct* 36(8):507–514
- Akram MS (2010) Physical and numerical investigation of conglomeratic rocks. Ph.D. thesis. Univ New South Wales, Sydney, Australia

- Bayram E, Tekin Y, Gokhan K (2014) Strength and ultrasonic properties of cemented paste backfill. *Ultrasonics* 54:195–204
- Button E, Riedmueller G, Schubert W, Klima K, Medley E (2004) Tunnelling in tectonic melanges-accommodating the impacts of geomechanical complexities and anisotropic rock mass fabrics. *Bull Eng Geol Environ* 63(2):109–117. <https://doi.org/10.1007/s10064-003-0220-7>
- Cen D, Huang D, Ren F (2017) Shear deformation and strength of the interphase between the soil–rock mixture and the benched bedrock slope surface. *Acta Geotech* 12(2):391–413
- Coli N, Berry P, Boldini D (2011) In situ non-conventional shear tests for the mechanical characterisation of a bimrock. *Int J Rock Mech Min* 48:95–102
- Donaghe RT, Torrey VH (1994) Proposed new standard test method for laboratory compaction testing of soil-rock mixtures using standard effort. *Geotech Test J* 3:387–392
- Du YN, Xu PF, Liang SQ (2018) Microtremor survey of soil-rock mixture landslides : an example of Baidian township, Hengyang City. *Chin J Geophys Chin Ed* 61(4):1596–1604
- Hartmut K (2001) Measuring and modeling of P- and S-wave velocities on crustal rocks: a key for the interpretation of seismic reflection and refraction data. *Int J Geo* 9:1–10
- Kahraman S (2002) Estimating the direct P-wave velocity value of intact rock from indirect laboratory measurements. *Int J Rock Mech Min* 39(1):101–104
- Kahraman S, Alber M, Fener M, Gunaydin O (2015) An assessment on the indirect determination of the volumetric block proportion of Misis fault breccia (Adana, Turkey). *Bull Eng Geol Environ* 74(3): 899–907
- Kalender A, Sonmez H, Medley E, Tunusluoglu C, Kasapoglu KE (2014) An approach to predicting the overall strengths of unwelded bimrocks and bimsoils. *Eng Geol* 183:65–79
- Kem H, Tubia JM (1993) Pressure and temperature dependence of P-and S-wave velocities, seismic anisotropy of sheared rocks from the Sierra Alpujata massif (Ronda peridotites, southern Spain). *Earth Planet Sci Lett* 119(23):191–205
- Kim C, Smell C, Medley E (2004) Shear strength of franciscan complex melange as calculated from back analysis of a landslide. In: *Proceedings of the Fifth International Conference on Case Histories in Geotechnical Engineering*, New York, pp 13–17
- Lindquist ES (1994) The strength and deformation properties of melange. Ph.D. Thesis, Department of Civil Engineering, University of California, Berkeley
- Lindquist ES, Goodman RE (1994) The strength and deformation properties of a physical model mélange. *Proc. 1st north American rock Mech. Symp.*, Austin, Texas, pp 843–850
- Mahdevari S, Maarefvand P (2017) Applying ultrasonic waves to evaluate the volumetric block proportion of bimrocks. *Arab J Geosci* 10(9):204
- Medley EW (1994) The engineering characterization of melanges and similar block-in-matrix rocks (bimrocks). Ph.D. Dissertation University of California at Berkeley
- Medley EW, Zekkos D (2011) Geopractitioner approaches to working with antisocial Mélanges. Invited paper. [Paper]. In: Wakabayashi J, Dilek Y (eds) *Mélanges: Processes of Formation and Societal Significance*, vol 480. Geological Society of America Special, pp 261–277
- MWRPRC (Ministry of Water Resources of the People's Republic of China) (1999) GB/T 50123–1999: standard for soil test method. MWRPRC, Beijing
- Napoli ML, Barbero M, Ravera E, Scavia C (2018) A stochastic approach to slope stability analysis in bimrocks. *Int J Rock Mech Min Sci* 101: 41–49
- Priyadarshree A, Kumar A, Gupta D, Pushkarna P (2018) Compaction and strength behavior of Tire crumbles–Fly ash mixed with clay. *J Mater Civ Eng* 30(4):04018033
- Slatalla N, Alber M, Kahraman S (2010) Analyses of acoustic emission response of a fault breccia in uniaxial deformation. *Bull Eng Geol Environ* 69(3):455–463
- Sonmez H, Tuncay E, Gokceoglu C (2004) Models to predict the uniaxial compressive strength and the modulus of elasticity for Ankara agglomerate. *Int J Rock Mech Min Sci* 41(5):717–729
- Sonmez H, Gokceoglu C, Medley E, Tuncay E, Nefeslioglu HA (2006) Estimating the uniaxial compressive strength of a volcanic bimrock. *Int J Rock Mech Min Sci* 43:554–561
- Su H, Hu J, Tong J, Wen Z (2012) Rate effect on mechanical properties of hydraulic concrete flexural-tensile specimens under low loading rates using acoustic emission technique. *Ultrasonics* 52(7):890–904
- Tsesarsky M, Hazan M, Gal E (2016) Estimating the elastic moduli and isotropy of block in matrix (bim) rocks by computational homogenization. *Eng Geol* 200:58–65
- Tsiambaos G (2010) Engineering Geological Behaviour of Heterogeneous and Chaotic Rock Masses. In: *Proceedings of the 12th International Congress. Bulletin of the Geological Society of Greece*, Patras. <https://doi.org/10.12681/bgsg.11173>
- Wang Y, Li X (2015) Experimental study on cracking damage characteristics of a soil and rock mixture by UPV testing. *Bull Eng Geol Environ* 74(3):775–788
- Wang Y, Li X, Zhang B, Wu YF (2014) Meso-damage cracking characteristics analysis for rock and soil aggregate with CT test. *SCIENCE CHINA Technol Sci* 57(7):1361–1371
- Wang Y, Li X, Hu RL, Li SD, Wang JY (2015) Experimental study of the ultrasonic and mechanical properties of SRM under compressive loading. *Environ Earth Sci* 74(6):5023–5037
- Wang Y, Li X, Zheng B, He JM, Li SD (2016) Macro–meso failure mechanism of soil–rock mixture at medium strain rates. *Géotechnique Lett* 6:235–243
- Wang Y, Li CH, Wei XM, Hou ZQ (2017a) Laboratory investigation of the effect of slenderness effect on the non-Darcy groundwater flow characteristics in Bimsoils. *Water* 9(9):676
- Wang Y, Li CH, Wei XM (2017b) Investigation of the macro–meso failure mechanism for soil–rock mixture under splitting loading using real-time ultrasonic measurement and 3-D laser scanning. *Eur J Environ Civ Eng*. <https://doi.org/10.1080/19648189.2017.1374882>
- Wang Y, Li CH, Hu YZ (2018) Use of X-ray computed tomography to investigate the effect of rock blocks on meso-structural changes in soil-rock mixture under triaxial deformation. *Constr Build Mater* 164:386–399
- Yamamoto Y, Springman SM (2017) Three-and four-point bending tests on artificial frozen soil samples at temperatures close to 0° C. *Cold Reg Sci Technol* 134:20–32
- Yasar E, Erdogan Y (2004) Correlating sound velocity with density, compressive strength and young modulus of carbonate rocks. *Int J Rock Mech Min* 41(5):871–875
- Yongbo F, Adewuyi OI, Chun F (2015) Strength characteristics of soil rock mixture under equal stress and cyclic loading conditions. *Geosyst Eng* 18(1):73–77
- Zhang LJ (2016) Study on time-lagged fracture characteristic of brittle rock under high stress condition. Ph.D. Dissertation China University of Geoscience in Wuhan
- Zhang S, Tang H, Zhan H, Lei G, Cheng H (2015) Investigation of scale effect of numerical unconfined compression strengths of virtual colluvial–deluvial soil–rock mixture. *Int J Rock Mech Min Sci* 77: 208–219
- Zhang ZL, Xu WJ, Xia W, Zhang HY (2016) Large-scale in-situ test for mechanical characterization of soil–rock mixture used in an embankment dam. *Int J Rock Mech Min Sci* 86:317–322